symmetry

MDPI

Article

Distributed Event-Triggered Control for Manipulator with Fixed-Time Disturbance Observer

Jing Pan [1], Gang Zhang [1,2,*], Duansong Wang [2] and Tianli Li [1]

[1] School of Electrical Engineering, Anhui Polytechnic University, Wuhu 241000, China; jingpan1102@126.com (J.P.); 2021030019@mail.wxc.edu.cn (T.L.)
[2] Anhui Undergrowth Crop Intelligent Equipment Engineering Research Center, Lu'an 237012, China; dswangsd@126.com
* Correspondence: zhanggang@wxc.edu.cn

Abstract: This article studies an event-triggered fixed-time trajectory tracking control problem of an n-joint manipulator system. Firstly, a fixed-time disturbance observer is proposed to reconstruct the total disturbance composed of external disturbances and model uncertainties, using the estimation as feedforward compensation to enhance the system robustness. Subsequently, based on the back-stepping framework, a fixed-time controller with an event-triggering mechanism is designed for the manipulator to ensure the convergence of tracking errors to zero within a fixed time. Additionally, two event-triggering conditions are devised to reduce the transmission time of control input and the computation time of control output. Simultaneously, Zeno behavior is excluded through theoretical proof, validating the fixed-time stability of the closed-loop system. Finally, simulation verification is conducted on a two-joint manipulator, with results confirming the effectiveness of the control strategy.

Keywords: n-joint manipulator system; trajectory tracking control; disturbance observer; event-triggered; fixed-time stability

check for updates

Citation: Pan, J.; Zhang, G.; Wang, D.; Li, T. Distributed Event-Triggered Control for Manipulator with Fixed-Time Disturbance Observer. *Symmetry* **2024**, *16*, 426. https://doi.org/10.3390/sym16040426

Academic Editor: Christos Volos

Received: 14 March 2024
Revised: 31 March 2024
Accepted: 1 April 2024
Published: 3 April 2024

Copyright: © 2024 by the authors. Licensee MDPI, Basel, Switzerland. This article is an open access article distributed under the terms and conditions of the Creative Commons Attribution (CC BY) license (https://creativecommons.org/licenses/by/4.0/).

1. Introduction

In recent years, rapid advancements in robotics technology have led to the widespread adoption of robots in industries, healthcare, military, aviation, and various other sectors, positioning them as a pivotal technology for the future growth of emerging industries. Within the robotics domain, the manipulator control system stands out as a highly competitive core technology. Developing a robotic arm control algorithm with superior tracking accuracy, fast convergence speed, and better control effect is important in engineering [1,2].

Robot control systems are inherently nonlinear and prone to external disturbances and model uncertainties, posing significant challenges for the design of the manipulator control systems. To enable manipulators to perform trajectory-tracking tasks quickly and accurately, scholars have proposed various control methods such as neural network control [3], fuzzy control [4], backstepping control [5], sliding mode control [6], event-triggered control [7], and disturbance observer-based control [8]. The method based on disturbance observer control has garnered considerable attention in recent years as it can enhance system control performance by identifying and compensating for lumped disturbances within the system. This method is known for its robustness. Many articles have been published on this control method. In [9], a disturbance observer-based adaptive fuzzy control method is introduced to address uncertain multi-input multi-output mechanical systems with unknown input nonlinearity. This method demonstrates that input nonlinearity can be decomposed into nominal parts and nonlinear disturbance terms. By employing a fuzzy logic system to mitigate model uncertainties and incorporating disturbance observers in the control design to handle fuzzy approximation errors, external disturbances, and nonlinear disturbances stemming from unknown input nonlinearity, the system's control performance can be improved. Another control strategy in [10] utilizes disturbance observer compensation to

tackle uncertainties in manipulator systems. By accurately estimating system uncertainties and providing feedforward compensation, the system's robustness is enhanced. However, these approaches often assume knowledge of the upper bound of total disturbances or impose restrictive assumptions such as the convergence of its time derivative.

In addition, in practical applications, computing and communication resources are often limited, making energy conservation crucial. Therefore, saving communication bandwidth and reducing computational load are highly practical considerations. Event-triggered control (ETC) involves triggering specific responses or actions based on external events, rather than at fixed time intervals. This approach allows for flexible real-time adjustments to system behavior through event perception, recognition, decision-making, and control strategies, resulting in a reduction of communication burden. ETC has gained significant attention from scholars in recent years. For instance, in [11], a combination of event-triggering mechanisms and adaptive neural networks is proposed for enhancing system tracking performance and reducing communication burden in the tracking control of flexible joint robots with random noise. The study in [12] focuses on the tracking control of manipulators with output constraints. An innovative finite-time adaptive event-triggered command filtering backstepping control method is introduced, utilizing command filtering to prevent direct differentiation of virtual control signals and compensation mechanisms to address filtering errors effectively. Moreover, the application of a relative threshold event-triggering mechanism aids in reducing resource waste and communication burden. In [13], a method for controlling unknown discrete-time nonlinear multi-agent systems (MASs) has been developed, utilizing a data-driven event-triggered approach. The method is based on Model-Free Adaptive Control (MFAC) to establish event-triggering conditions for MASs to reduce controller update time. Additionally, a unified quantization mechanism is designed for encoding and decoding to compress the communication data volume between intelligent agents. A novel event-triggered MFAC algorithm is introduced for MASs featuring unified quantization, operating solely on data without dependence on system model or structure information. In [14], an event-triggered impulsive control is applied to image encryption technology based on fractal interpolation for variable-order fractional chaotic Lur'e systems. It achieves synchronization through event-triggered impulsive control, coupled with short-term memory mechanisms. In [15], the synchronization problem of inertial neural networks (INNs) with time delay using event-triggered (E-T) impulsive control is studied. The control input is only required at triggered instants, this method can effectively improve system performance. In [16], the synchronization problem of delayed chaotic neural networks with impulsive control, event-triggered impulsive control, and event-triggered delayed impulsive control is investigated. This method can construct an event-triggering mechanism based on Lyapunov to derive sufficient conditions for linear matrix inequality (LMI).

However, the convergence time of the aforementioned control methods is typically dependent on the initial error of the system. The greater the initial error, the more prolonged the convergence time. In practical applications, stringent time response is necessary to ensure system error stability within a finite time and that the convergence time is independent of the initial state of the system. Fixed-time control (FTC) has been thoroughly studied by scholars in recent years, yielding significant advancements. The problem of fixed-time adaptive trajectory tracking control for quadcopter unmanned aerial vehicles (QUAVs) with error constraints is addressed in [17]. Through the utilization of a fixed-time command filter, the "explosion of complexity" (EOC) phenomenon in traditional backstepping control methods has been successfully resolved. Additionally, a novel fractional power error compensation mechanism has effectively mitigated the impact of filtering errors. A fixed-time adaptive control method is formulated by combining backstepping, prescribed performance control, and command filtering technologies. The problem of singularity-free adaptive fuzzy fixed-time control for uncertain n-link robot systems with position tracking error constraints is explored in [18]. An improved error conversion mechanism based on performance functions has been proposed, constraining the converted error to an interval

greater than zero and developing a suitable barrier Lyapunov function (BLF) to prevent violations of position tracking error constraints. In comparison to existing methods, the proposed adaptive fixed-time controller avoids singularity issues in backstepping-based fixed-time control design and ensures rapid transient response. To address the three main challenges of fault-tolerant control for robotic arms in [19]: (1) Model-based fault-tolerant control design necessitates partial or complete knowledge of robot dynamics. (2) Fault-tolerant control exhibits enhanced robustness, reduced flutter, lower tracking error, and faster response rate. (3) Global fixed-time system convergence. A self-adaptive fuzzy backstepping control scheme has been developed to enhance system tracking performance. This approach does not require full prior knowledge of the robot dynamics model, facilitating practical controller implementation. Moreover, the system tracking error converges within a fixed time, providing system performance information in advance.

To solve the above problems and achieve fast and accurate tracking control of the manipulator, this article proposes a fixed-time controller based on the event-triggering mechanism for the manipulator. The main contributions are summarized as follows:

(1) To address the impact of total disturbance on the control system of a manipulator, this article designs a disturbance observer that can accurately reconstruct the lumped disturbance within a fixed time, independent of the system's initial state. Additionally, unlike previous works in [10], restrictive assumptions such as the upper bound of the total disturbance being known or its time derivative converging are all relaxed.
(2) The introduction of the event-triggering mechanism effectively conserves communication and computing resources. Specifically, within the framework of backstepping, a fixed-time controller for the manipulator based on the event-triggering mechanism is developed, which significantly reduces the transmission time of control inputs and the calculation time of control outputs.
(3) By combining the event-triggering mechanism with fixed-time control theory, the controller can effectively leverage the benefits of ETC and FTC through the selection of an appropriate event-triggering parameter and control parameter which enables the manipulator to track the desired trajectory within a fixed time while conserving communication resources.

2. Preliminaries

2.1. Notations

In this article, the following notations will be used: $\mathbb{R}$ represents the set of real numbers and $\mathbb{R}_+$ represents a set of positive real numbers. $\mathbb{R}^n$ denotes the Euclidean space with dimension n, and $\mathbb{R}^{n\times n}$ denotes the space of all $n \times n$ matrices. For any non-negative real number $\alpha \in \mathbb{R}_+$, we define $\chi \mapsto sig^{\alpha}(\chi)$ as $sig^{\alpha}(\chi) = sign(\chi)|\chi|^{\alpha}$ for any $\chi \in \mathbb{R}$, $sign(\chi)$ is the standard signum function, $|.|$ denotes the absolute value, and $I^{n\times 1}$ is an $n \times 1$ matrix whose elements are all 1.

2.2. Problem Formation

Considering an n-link manipulator, the motion equations are given by [20,21]:

$$M(q)\ddot{q} + C(q,\dot{q})\dot{q} + G(q) = \tau(t) - J^T(q)f(t) \tag{1}$$

where q, $\dot{q}$, and $\ddot{q} \in \mathbb{R}^n$ respectively represent position vector, velocity vector, and acceleration vector. $M(q) \in \mathbb{R}^{n\times n}$ is a symmetric positive definite inertia matrix. $C(q,\dot{q}) \in \mathbb{R}^{n\times n}$ denotes the Coriolis and centripetal force matrix. $G(q) \in \mathbb{R}^n$ is the gravitational matrix, and $\tau(t) \in \mathbb{R}^n$ represents the control input vector. $J(q)$ is the Jacobian matrix. $f(t) \in \mathbb{R}^n$ represents the vector of the constrained force exerted by the environment and humans.

When the model uncertainty is considered, to facilitate control design, let

$$\begin{cases} x = q \\ \nu = \dot{q} \end{cases} \tag{2}$$

In accordance with (1) and (2), we have

$$\begin{cases} \dot{x} = \nu \\ \dot{\nu} = M^{-1}(x)[\tau(t) - C(x,\nu)\nu - G(x) + \varpi] \end{cases} \tag{3}$$

where ϖ denotes the lumped disturbance of the manipulator, which is composed of external disturbances and model uncertainties. Its expression is as follows:

$$\varpi = -\Delta C(x,\nu)\nu - \Delta G(x) - J^T(x)f(t) \tag{4}$$

where $\Delta C(x,\nu)$ and $\Delta G(x)$ represent the uncertainty dynamic.

Then, in accordance with (3), the trajectory of tracking can be depicted as follows:

$$\begin{cases} \dot{x}_d = \nu_d \\ \dot{\nu}_d = M_d^{-1}(x)[\tau_d(t) - C(x_d,\nu_d)\nu_d - G(x_d)] \end{cases} \tag{5}$$

where $x_d = \begin{bmatrix} q_{d1} & q_{d2} \dots & q_{dn} \end{bmatrix}^T$ and $\nu_d = \begin{bmatrix} \dot{q}_{d1} & \dot{q}_{d2} \dots & \dot{q}_{dn} \end{bmatrix}^T$ represent the expected position and velocity vector, respectively. $\tau_d(t) - C(x_d,\nu_d)\nu_d - G(x_d)$ denotes the desired dynamics.

Control Objective: Considering model uncertainties and external disturbances for model (3), a fixed-time disturbance observer is formulated to precisely estimate the lumped disturbance and provide compensation for the manipulator system. Simultaneously, by combining backstepping, fixed-time control theory, and a distributed event-triggering mechanism. A trajectory-tracking control law is designed for the manipulator, which ensures the manipulator tracks the desired trajectory within a fixed time while ensuring all closed-loop signals achieve global fixed-time stability. The mathematical expressions can be written as follows:

$$\lim_{t \to T} \|x - x_d\| = 0 \tag{6}$$

where $T \in [0, +\infty)$ denotes the convergence time.

2.3. Lemmas

To achieve the control objectives, the following lemmas are essential.

Lemma 1. *Consider the following system [22,23]:*

$$\begin{cases} \dot{x}_1 = x_2 \\ \dot{x}_2 = \nu_{nom}(x_1, x_2) \end{cases} \tag{7}$$

where x_1 and $x_2 \in \mathbb{R}^n$ are state variables and $\nu_{nom} \in \mathbb{R}^n$ is the control input. If $\nu_{nom}(x_1, x_2)$ satisfies

$$\nu_{nom}(x_1,x_2) = -\left(\varepsilon_1 sig^{\gamma_1}(x_1) + \varepsilon_1' sig(x_1) + \varepsilon_1'' sig^{\gamma_1'}(x_1)\right) - \left(\varepsilon_2 sig^{\gamma_2}(x_2) + \varepsilon_2' sig(x_2) + \varepsilon_2'' sig^{\gamma_2'}(x_2)\right) \tag{8}$$

where $\varepsilon_i > 0$, $\varepsilon_i' > 0$, $\varepsilon_i'' > 0$, $(i = 1, 2)$, $\gamma_1 = \frac{\gamma}{2-\gamma}$, $\gamma_2 = \gamma$, $\gamma_1' = \frac{4-3\gamma}{2-\gamma}$, $\gamma_2' = \frac{4-3\gamma}{3-2\gamma}$, $\gamma \in (0,1)$. Then, we have the following results:

(1) The origin of the closed-loop system (7) is fixed-time stable.

(2) The upper bound of convergence time T_e satisfies

$$T_e = \frac{2}{k_\nu(1-\nu_1)} + \frac{2}{k_\nu(\nu_2 - 1)} \tag{9}$$

where k_ν is a positive constant, $\nu_1 = \frac{d_{\nu 0} + k_{s0}}{d_{\nu 0}}$, $\nu_2 = \frac{d_{\nu\infty} + k_{s\infty}}{d_{\nu\infty}}$, $k_{s0} = -1$, $k_{s\infty} = 1$, $d_{\nu 0} = \max\left(\frac{2-\gamma}{1-\gamma}, \frac{1}{1-\gamma}\right)$, $d_{\nu\infty} = \max\left(\frac{2-\gamma}{1-\gamma}, \frac{3-2\gamma}{1-\gamma}\right)$.

Lemma 2. *If there exists a continuous radial bounded function* $V : \mathbb{R}^n \to \mathbb{R}_+ \cup \{0\}$ *[24], such that*

(1) $V(x) = 0 \Leftrightarrow x = 0$.

(2) for any $x(t)$ *satisfies the following inequality:*

$$\dot{V}(x) \leq -\alpha V^p(x) - \beta V^q(x) \tag{10}$$

Then, the system is fixed-time stable, where α, β, p, *and* q *are positive constants, and* $0 < p < 1$, $q > 1$. *The settling time is bounded by* T:

$$T \leq T_{\max} := \frac{1}{\alpha(1-p)} + \frac{1}{\beta(q-1)} \tag{11}$$

Lemma 3. *If* $\iota_1, \iota_2 \ldots \iota_M \geq 0$, *there exists the following inequality [25]:*

$$\begin{cases} \sum\limits_{i=1}^{M} \iota_i^k \geq \left(\sum\limits_{i=1}^{M} \iota_i \right)^k & 0 < k \leq 1 \\ \sum\limits_{i=1}^{M} \iota_i^k \geq M^{1-k} \left(\sum\limits_{i=1}^{M} \iota_i \right)^k & 1 < k < \infty \end{cases} \tag{12}$$

3. Controller Design

3.1. Observer Design

This section is based on the concept of an unknown input observer [26] and proposes a fixed-time nonlinear disturbance observer for precise estimation of the lumped disturbance. The specific design process is as follows:

In accordance with (3), we have

$$\dot{\nu} = -\lambda_1 \nu + M^{-1}(x)\tau(t) + \varpi_{lump} \tag{13}$$

where $\lambda_1 > 0$, $\varpi_{lump} = \Phi(x, \nu) + \lambda_1 \nu + M^{-1}(x)\varpi$, $\Phi(x, \nu) = M^{-1}(x)(-C(x, \nu) - G(x))$. For the dynamical system (13), we introduce the following auxiliary system for constructing an unknown input linear system:

$$\ddot{x}_a = -\lambda_1 \dot{x}_a + M^{-1}(x)\tau(t) \tag{14}$$

where $x_a \in \mathbb{R}^n$ is the state of the auxiliary system (14). We define a new variable $\chi = x - x_a$ and take its time derivative to obtain the unknown input linear system as follows:

$$\begin{cases} \ddot{\chi} = -\lambda_1 \dot{\chi} + \varpi_{lump} \\ y = \lambda_2 \dot{\chi} \end{cases} \tag{15}$$

where $\lambda_2 > 0$, χ is the state of the system, ϖ_{lump} is an unknown input, and y is the output of the system.

To facilitate the design, let $\chi_1 = \chi$, $\chi_2 = \dot{\chi}$, and (15) can be rewritten as follows:

$$\begin{cases} \dot{\chi}_1 = \chi_2 \\ \dot{\chi}_2 = -\lambda_1 \chi_2 + \varpi_{lump} \\ y = \lambda_2 \chi_2 \end{cases} \tag{16}$$

Then, a fixed-time disturbance observer can be designed as follows:

$$\begin{cases} \dot{\hat{\chi}}_1 = \hat{\chi}_2 \\ \dot{\hat{\chi}}_2 = \frac{1}{\lambda_2} \dot{y} + \nu_{noms}(\chi_{e1}, \chi_{e2}) \end{cases} \tag{17}$$

where $\chi_{e1} = \chi_1 - \hat{\chi}_1 \chi_{e2} = \chi_2 - \hat{\chi}_2, \nu_{noms}(\chi_{e1}, \chi_{e2}) = \left(\varepsilon_1 sig^{\gamma_1}(\chi_{e1}) + \varepsilon_1' sig(\chi_{e1}) + \varepsilon_1'' sig^{\gamma_1'}(\chi_{e1})\right) + \left(\varepsilon_2 sig^{\gamma_2}(\chi_{e2}) + \varepsilon_2' sig(\chi_{e2}) + \varepsilon_2'' sig^{\gamma_2'}(\chi_{e2})\right)$, $\varepsilon_i > 0$, $\varepsilon_i' > 0$, $\varepsilon_i'' > 0$, $(i = 1,2)$, $\gamma_1 = \frac{\gamma}{2-\gamma}$, $\gamma_2 = \gamma$, $\gamma_1' = \frac{4-3\gamma}{2-\gamma}$, $\gamma_2' = \frac{4-3\gamma}{3-2\gamma}$, $\gamma \in (0,1)$.

Theorem 1. *For (16), if the disturbance observer is designed as (17), then, it can be guaranteed that the unknown input ϖ_{lump} can be estimated by $\hat{\varpi}_{lump}$ within a fixed time T_e. $\hat{\varpi}_{lump}$ can be obtained from Equation (18).*

$$\hat{\varpi}_{lump} = \lambda_1 \hat{\chi}_2 + \frac{1}{\lambda_2} \dot{y} \tag{18}$$

Then, ϖ can be reconstructed by $\hat{\varpi}$, which can be obtained by (19):

$$\hat{\varpi} = M(x)\left(\hat{\varpi}_{lump} - \lambda_1 \nu - \Phi(x, \nu)\right) \tag{19}$$

Proof of Theorem 1. Combining (16) and (17), we have

$$\begin{cases} \dot{\chi}_{e1} = \chi_{e2} \\ \dot{\chi}_{e2} = \dot{\chi}_2 - \frac{1}{\lambda_2}\dot{y} - \nu_{noms}(\chi_{e1}, \chi_{e2}) = -\nu_{noms}(\chi_{e1}, \chi_{e2}) \end{cases} \tag{20}$$

In accordance with Lemma 1, we can know that χ_{e1} and χ_{e2} can converge to zero within a fixed time, and the convergence time T_e is given by

$$T_e = \frac{2}{k_\nu(1-\nu_1)} + \frac{2}{k_\nu(\nu_2 - 1)} \tag{21}$$

where k_ν is a positive constant, $\nu_1 = \frac{d_{\nu 0} + k_{s0}}{d_{\nu 0}}$, $\nu_2 = \frac{d_{\nu\infty} + k_{s\infty}}{d_{\nu\infty}}$, $k_{s0} = -1$, $k_{s\infty} = 1$, $d_{\nu 0} = \max\left(\frac{2-\gamma}{1-\gamma}, \frac{1}{1-\gamma}\right)$, $d_{\nu\infty} = \max\left(\frac{2-\gamma}{1-\gamma}, \frac{3-2\gamma}{1-\gamma}\right)$. When $t \geq T_e$, we have $\chi_{e1} = \chi_{e2} = 0$. Now, define the estimation error $\widetilde{\varpi}_{lump} = \varpi_{lump} - \hat{\varpi}_{lump}$. Combining (16) and (18), we have

$$\widetilde{\varpi}_{lump} = \dot{\chi}_2 + \lambda_1 \chi_2 - \lambda_1 \hat{\chi}_2 - \frac{1}{\lambda_2}\dot{y} = \lambda_1 \chi_{e1} \tag{22}$$

In accordance with (22), we can further conclude that $\widetilde{\varpi}_{lump}$ is fixed-time convergence. Defining $\varpi_e = \varpi - \hat{\varpi}$ and combining with (16), (18), and (19), we have

$$\begin{aligned} \varpi_e &= M(x)\left(\varpi_{lump} - \Phi(x,\nu) - \lambda_1 \nu\right) - M(x)\left(\hat{\varpi}_{lump} - \lambda_1 \nu - \Phi(x,\nu)\right) \\ &= M(x)\left(\varpi_{lump} - \hat{\varpi}_{lump}\right) \\ &= M(x)\left(\varpi_{lump} - \lambda_1 \hat{\chi}_2 - \tfrac{1}{\lambda_2}\dot{y}\right) \\ &= M(x)\left(\varpi_{lump} - \lambda_1 \hat{\chi}_2 - \left(-\lambda_1 \chi_2 + \varpi_{lump}\right)\right) \\ &= M(x)\lambda_1(\chi_2 - \hat{\chi}_2) \\ &= M(x)\lambda_1 \chi_{e2} \end{aligned} \tag{23}$$

In accordance with (23), when $t \geq T_e$, we have $\varpi_e = 0$, and it is proved that ϖ can be accurately estimated by $\hat{\varpi}$. □

3.2. Controller Design

The trajectory tracking diagram of the manipulator is shown in Figure 1.

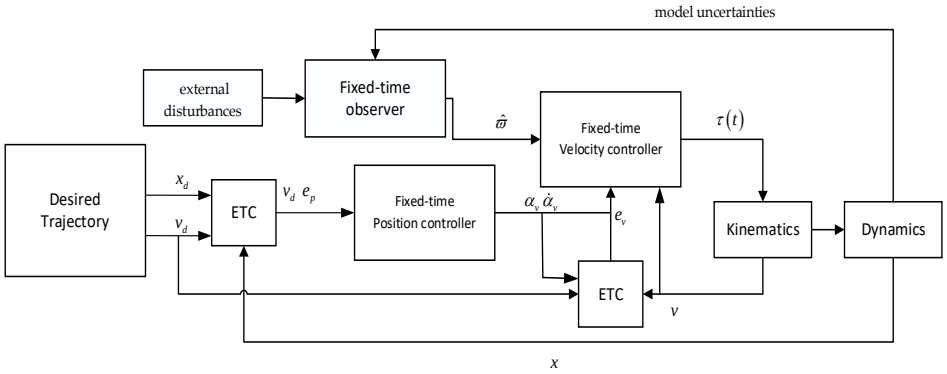


Figure 1. A diagram of the manipulator tracking control.

Define the position-tracking error $e_p \in \mathbb{R}^n$ of the manipulator as follows:

$$e_p = x - x_d \tag{24}$$

In accordance with (3) and (5), the time derivative of (24) is

$$\dot{e}_p = v - v_d \tag{25}$$

Based on the event-triggered mechanism, the kinematic controller α_v is designed as follows:

$$\alpha_v = v_d - sign\big(e_p(t_k)\big)\Big(k_1\big|e_p(t_k)\big|^{2-m/n} + k_2\big|e_p(t_k)\big|^{m/n} + k_3\big|e_p(t_k)\big| + k_4 I^{n\times 1}\Big) \tag{26}$$

where m, n are positive constants with $m < n$. $k_1 = diag[k_{1,1}, \ldots, k_{1,n}]$, $k_2 = diag[k_{2,1}, \ldots, k_{2,n}]$, $k_3 = diag[k_{3,1}, \ldots, k_{3,n}]$, $k_4 = diag[k_{4,1}, \ldots, k_{4,n}]$ with $k_{1,\delta}, k_{2,\delta}, k_{3,\delta}, k_{4,\delta} > 0$, $(\delta = 1, 2, \ldots, n)$. δ is the symbol of an element in the vector.

Now, to design this event-triggering mechanism, the measurement error z_p is defined as follows:

$$\begin{aligned} z_p(t) = {} & sign\big(e_p(t)\big)\Big(-k_1\big|e_p(t)\big|^{2-m/n} - k_2\big|e_p(t)\big|^{m/n} - k_3\big|e_p(t)\big| - k_4 I^{n\times 1}\Big) \\ & -sign\big(e_p(t_k)\big)\Big(-k_1\big|e_p(t_k)\big|^{2-m/n} - k_2\big|e_p(t_k)\big|^{m/n} - k_3\big|e_p(t_k)\big| - k_4 I^{n\times 1}\Big) \end{aligned} \tag{27}$$

Then, the event-triggered function for the manipulator is designed as follows:

$$\Upsilon_{p,\delta}(t) = \big|z_{p,\delta}(t)\big| - \rho_{p,\delta}\Big(k_{1,\delta}\big|e_{p,\delta}(t)\big|^{2-m/n} + k_{2,\delta}\big|e_{p,\delta}(t)\big|^{m/n} + k_{3,\delta}\big|e_{p,\delta}(t)\big|\Big) - k_{4,\delta} \tag{28}$$

where $\rho_{p,\delta} \in (0,1)$ is the triggering parameter that determines the frequency of the event-triggered function.

For manipulator systems, the triggering time of the kinematic controller is determined by $\Upsilon_{p,\delta}(t)$ and defines the event-triggering mechanism as follows:

$$t_{p,k+1} = \inf\big\{t > t_k : \exists \Upsilon_{p,\delta}(t) \geq 0; k \in N\big\}, t_0 = 0 \tag{29}$$

where $t_0 \ldots t_k, t_{k+1}$ is the event-trigger time series, when t_k arrives, $\Upsilon_{p,\delta}(t) \geq 0$, and (29) is triggered to update the kinematic controller α_v.

To verify the convergence of e_p, choose the Lyapunov function candidate as

$$V_1 = \frac{1}{2}e_p^T e_p = \sum_{\delta=1}^{n}\frac{1}{2}e_{p,\delta}^2 \tag{30}$$

Then, the time derivative of V_1 is as follows:

$$\begin{aligned} \dot{V}_1 &= e_p^T \dot{e}_p \\ &= e_p^T (\nu - \nu_d) \end{aligned} \tag{31}$$

Substituting (26) into (31), we have

$$\begin{aligned} \dot{V}_1 &= e_p^T \Big(-sign\big(e_p(t_k)\big) \Big(k_1 \big|e_p(t_k)\big|^{2-m/n} + k_2 \big|e_p(t_k)\big|^{m/n} + k_3 \big|e_p(t_k)\big| + k_4 I^{n\times 1} \Big) \Big) \\ &= e_p^T \Big(-z_p(t) - sign\big(e_p(t)\big) \Big(k_1 \big|e_p(t)\big|^{2-m/n} + k_2 \big|e_p(t)\big|^{m/n} + k_3 \big|e_p(t)\big| + k_4 I^{n\times 1} \Big) \Big) \\ &\le \sum_{\delta=1}^{n} |e_{p,\delta}||z_{p,\delta}(t)| - e_p^T sign\big(e_p(t)\big) \Big(k_1 \big|e_p\big|^{2-m/n} + k_2 \big|e_p\big|^{m/n} + k_3 \big|e_p\big| + k_4 I^{n\times 1} \Big) \\ &\le \sum_{\delta=1}^{n} \Big(\rho_{p,\delta} |e_{p,\delta}| \Big(k_{1,\delta} \big|e_{p,\delta}\big|^{2-m/n} + k_{2,\delta} \big|e_{p,\delta}\big|^{m/n} + k_{3,\delta} \big|e_{p,\delta}\big| \Big) + k_{4,\delta} |e_{p,\delta}| \\ &\qquad -k_{1,\delta} 2^{\frac{3-m/n}{2}} \Big(\tfrac{1}{2} e_{p,\delta}^2 \Big)^{\frac{3-m/n}{2}} - k_{2,\delta} 2^{\frac{1+m/n}{2}} \Big(\tfrac{1}{2} e_{p,\delta}^2 \Big)^{\frac{1+m/n}{2}} - k_{3,\delta} e_{p,\delta}^2 - k_{4,\delta} |e_{p,\delta}| \Big) \\ &\le \sum_{\delta=1}^{n} (\rho_{p,\delta} - 1) k_{1,\delta} 2^{\frac{3-m/n}{2}} \Big(\tfrac{1}{2} e_{p,\delta}^2 \Big)^{\frac{3-m/n}{2}} + (\rho_{p,\delta} - 1) k_{2,\delta} 2^{\frac{1+m/n}{2}} \Big(\tfrac{1}{2} e_{p,\delta}^2 \Big)^{\frac{1+m/n}{2}} \end{aligned} \tag{32}$$

Combining Lemma 3, the formula (32) can be further written as follows:

$$\dot{V}_1 \le -\alpha_1 V_1^{\frac{3n-m}{2n}} - \beta_1 V_1^{\frac{n+m}{2n}} \tag{33}$$

where $\alpha_1 = \min\Big((1-\rho_{p,\delta}) k_{1,\delta} 2^{\frac{3n-m}{2n}} \Big) n^{\frac{m-n}{2n}}$, $\beta_1 = \min\Big((1-\rho_{p,\delta}) k_{2,\delta} 2^{\frac{1+m/n}{2n}} \Big)$.

In accordance with Lemma 2, the position tracking error e_p can be reduced to zero within a fixed time.

The output of the fixed-time position/attitude controller can be regarded as the desired linear and angular velocities of the manipulator. To minimize the error between the actual linear/angular velocities and the desired linear/angular velocities of the manipulator, we will design a fixed-time linear/angular velocities controller for the manipulator.

Define the speed-tracking error of the manipulator as follows:

$$e_\nu = \nu - \alpha_\nu \tag{34}$$

In accordance with (3), the time derivative of e_ν can be obtained as:

$$\dot{e}_\nu = M^{-1}(x)[\tau(t) - C(x,\nu)\nu - G(x) + \varpi] - \dot{\alpha}_\nu \tag{35}$$

The manipulator system's control strategy $\tau(t)$ can be formulated as follows:

$$\begin{aligned} \tau(t) = M(x) \Big(& -k_5 sign(e_\nu(t_k)) |e_\nu(t_k)|^{2-m/n} - k_6 sign(e_\nu(t_k)) |e_\nu(t_k)|^{m/n} - k_7 sign(e_\nu(t_k)) |e_\nu(t_k)| \\ & -k_8 sign(e_\nu(t_k)) I^{n\times 1} + \dot{\alpha}_\nu \Big) + C(x,\nu)\nu + G(x) - \hat{\varpi} \end{aligned} \tag{36}$$

where $k_5 = diag[k_{5,1}, \ldots, k_{5,n}]$, $k_6 = diag[k_{6,1}, \ldots, k_{6,n}]$, $k_7 = diag[k_{7,1}, \ldots, k_{7,n}]$, $k_8 = diag[k_{8,1}, \ldots, k_{8,n}]$ with $k_{5,\delta}, k_{6,\delta}, k_{7,\delta}, k_{8,\delta} > 0$, $(\delta = 1, 2, \ldots, n)$.

Similar to the design of kinematic controllers α_ν, we define measurement errors as follows:

$$\begin{aligned} z_\nu(t) = & sign(e_\nu(t)) \Big(-k_5 |e_\nu(t)|^{2-m/n} - k_6 |e_\nu(t)|^{m/n} - k_7 |e_\nu(t)| - k_8 I^{n\times 1} \Big) \\ & -sign(e_\nu(t_k)) \Big(-k_5 |e_\nu(t_k)|^{2-m/n} - k_6 |e_\nu(t_k)|^{m/n} - k_7 |e_\nu(t_k)| - k_8 I^{n\times 1} \Big) \end{aligned} \tag{37}$$

Then, the event-triggered function can be designed as follows:

$$\gamma_{\nu,\delta}(t) = |z_{\nu,\delta}(t)| - \rho_{\nu,\delta} \Big(k_{5,\delta} |e_{\nu,\delta}(t)|^{2-m/n} + k_{6,\delta} |e_{\nu,\delta}(t)|^{m/n} + k_{7,\delta} |e_{\nu,\delta}(t)| \Big) - k_{8,\delta} \tag{38}$$

where $\rho_{\nu,\delta} \in (0,1)$ is the triggering parameter that determines the frequency of the event-triggered function.

Define the event-triggered mechanism as follows:

$$t_{\nu,k+1} = \inf\{t > t_k : \exists \Upsilon_{\nu,\delta}(t) \geq 0; k \in N\}, t_0 = 0 \tag{39}$$

when t_k arrives, $\Upsilon_{\nu,\delta}(t) \geq 0$, and (39) is triggered to update the status information of the manipulator.

To verify the convergence of e_ν, the following Lyapunov function is constructed:

$$V_2 = \frac{1}{2} e_\nu^T e_\nu = \sum_{\delta=1}^{n} \frac{1}{2} e_{\nu,\delta}^2 \tag{40}$$

Take the time derivative of V_2

$$\begin{aligned} \dot{V}_2 &= e_\nu^T \dot{e}_\nu \\ &= e_\nu^T \left(M^{-1}(x)[\tau(t) - C(x,\nu)\nu - G(x) + \varpi] - \dot{\alpha}_\nu \right) \end{aligned} \tag{41}$$

Substituting expression (36) into (41), (41) can be further simplified into the following form:

$$\dot{V}_2 = e_\nu^T \Big(-sign(e_\nu(t_k)) \Big(k_5 |e_\nu(t_k)|^{2-m/n} + k_6 |e_\nu(t_k)|^{m/n} + k_7 |e_\nu(t_k)| + k_8 I^{n\times 1} \Big) + M^{-1}(x)(\varpi - \hat{\varpi}) \Big) \tag{42}$$

In accordance with Theorem 1, when $t \geq T_e$, we have $\varpi_e = \varpi - \hat{\varpi} = 0$, and (42) can be further simplified as follows:

$$\begin{aligned} \dot{V}_2 &= e_\nu^T \Big(-sign(e_\nu(t_k)) \Big(k_5 |e_\nu(t_k)|^{2-m/n} + k_6 |e_\nu(t_k)|^{m/n} + k_7 |e_\nu(t_k)| + k_8 I^{n\times 1} \Big) \Big) \\ &= e_\nu^T \Big(-z_\nu(t) - sign(e_\nu(t)) \Big(k_5 |e_\nu(t)|^{2-m/n} + k_6 |e_\nu(t)|^{m/n} + k_7 |e_\nu(t)| + k_8 I^{n\times 1} \Big) \Big) \\ &\leq \sum_{\delta=1}^{n} |e_{\nu,\delta}||z_{\nu,\delta}(t)| - e_\nu^T sign(e_\nu(t)) \Big(k_5 |e_\nu|^{2-m/n} + k_6 |e_\nu|^{m/n} + k_7 |e_\nu| + k_8 I^{n\times 1} \Big) \\ &\leq \sum_{\delta=1}^{n} \Big(\rho_{\nu,\delta} |e_{\nu,\delta}| \Big(k_{5,\delta} |e_{\nu,\delta}|^{2-m/n} + k_{6,\delta} |e_{\nu,\delta}|^{m/n} + k_{7,\delta} |e_{\nu,\delta}| \Big) + k_{8,\delta} |e_{\nu,\delta}| \\ &\qquad - k_{5,\delta} 2^{\frac{3-m/n}{2}} \left(\frac{1}{2} e_{\nu,\delta}^2 \right)^{\frac{3-m/n}{2}} - k_{6,\delta} 2^{\frac{1+m/n}{2}} \left(\frac{1}{2} e_{\nu,\delta}^2 \right)^{\frac{1+m/n}{2}} - k_{7,\delta} e_{\nu,\delta}^2 - k_{8,\delta} |e_{\nu,\delta}| \Big) \\ &\leq \sum_{\delta=1}^{n} (\rho_{\nu,\delta} - 1) k_{5,\delta} 2^{\frac{3-m/n}{2}} \left(\frac{1}{2} e_{\nu,\delta}^2 \right)^{\frac{3-m/n}{2}} + (\rho_{\nu,\delta} - 1) k_{6,\delta} 2^{\frac{1+m/n}{2}} \left(\frac{1}{2} e_{\nu,\delta}^2 \right)^{\frac{1+m/n}{2}} \end{aligned} \tag{43}$$

In accordance with Lemma 3, the above formula can be rewritten as follows:

$$\dot{V}_2 \leq -\alpha_2 V_2^{\frac{3n-m}{2n}} - \beta_2 V_2^{\frac{n+m}{2n}} \tag{44}$$

where $\alpha_2 = \min\Big((1-\rho_{\nu,\delta}) k_{5,\delta} 2^{\frac{3n-m}{2n}} \Big) n^{\frac{m-n}{2n}}$, $\beta_2 = \min\Big((1-\rho_{\nu,\delta}) k_{6,\delta} 2^{\frac{1+m/n}{2n}} \Big)$.

In accordance with Lemma 2, the velocity tracking error e_ν can be reduced to zero within a fixed time.

Theorem 2. *Considering the manipulator model (1), the distributed event-triggering is introduced into the manipulator control strategy. Combined with a fixed-time disturbance observer (17), the designed control strategy (36) can enable the manipulator to track the desired trajectory within a fixed time, and the convergence time is independent of the initial state of the system.*

Proof. To verify the stability of the entire closed-loop system, the chosen Lyapunov function is as follows:

$$V_3 = V_1 + V_2 \tag{45}$$

Synthesize (31) and (41), the time derivative of (45):

$$\begin{aligned}\dot{V}_3 &= e_p\dot{e}_p + e_v\dot{e}_v \\ &\leq \sum_{\delta=1}^{n}(\rho_{p,\delta}-1)k_{1,\delta}2^{\frac{3-m/n}{2}}\left(\tfrac{1}{2}e_{p,\delta}^2\right)^{\frac{3-m/n}{2}} + (\rho_{p,\delta}-1)k_{2,\delta}2^{\frac{1+m/n}{2}}\left(\tfrac{1}{2}e_{p,\delta}^2\right)^{\frac{1+m/n}{2}} \\ &\quad + \sum_{\delta=1}^{n}(\rho_{v,\delta}-1)k_{5,\delta}2^{\frac{3-m/n}{2}}\left(\tfrac{1}{2}e_{v,\delta}^2\right)^{\frac{3-m/n}{2}} + (\rho_{v,\delta}-1)k_{6,\delta}2^{\frac{1+m/n}{2}}\left(\tfrac{1}{2}e_{v,\delta}^2\right)^{\frac{1+m/n}{2}}\end{aligned} \tag{46}$$

In accordance with (33), (44), and Lemma 3, we further have

$$\begin{aligned}\dot{V}_3 &\leq -\alpha_1 V_1^{\frac{3n-m}{2n}} - \beta_1 V_1^{\frac{n+m}{2n}} - \alpha_2 V_2^{\frac{3n-m}{2n}} - \beta_2 V_2^{\frac{n+m}{2n}} \\ &\leq -\min(\alpha_1,\alpha_2)2^{\frac{m-n}{2n}} V_3^{\frac{3n-m}{2n}} - \min(\beta_1,\beta_2)V_3^{\frac{n+m}{2n}} \\ &= -\alpha_3 V_3^{\frac{3n-m}{2n}} - \beta_3 V_3^{\frac{n+m}{2n}}\end{aligned} \tag{47}$$

where $\alpha_3 = \min(\alpha_1,\alpha_2)2^{\frac{m-n}{2n}}$, $\beta_3 = \min(\beta_1,\beta_2)$.

In accordance with Lemma 2, we can conclude that the event-triggered mechanism-based fixed-time control system for the manipulator proposed in this article is a fixed-time stable system, and the upper bound of convergence time T_s satisfies.

$$\begin{aligned}T_s \leq T_{\max}: &= \frac{1}{\alpha_3\left(\frac{3n-m}{2n}-1\right)} + \frac{1}{\beta_3\left(1-\frac{n+m}{2n}\right)} \\ &= \frac{2n}{n-m}\left(\frac{1}{\alpha_3}+\frac{1}{\beta_3}\right)\end{aligned} \tag{48}$$

and total convergence time $T_{es} \leq T_e + T_s$. □

3.3. Zeno Behavior Exclusion

The key to successfully designing an event-triggered controller is to eliminate the Zeno phenomenon; if there is Zeno behavior, it will cause the controller to be triggered infinitely within a finite time. If the difference value between two triggers $\{t_{k+1}-t_k, k\in N\}$ has a positive lower bound, this indicates that there is no Zeno behavior during the event-triggering process.

Theorem 3. *Consider the manipulator model (1), for any initial state, with the controller (36) and trigger conditions (29) and (39), and the difference value between two triggers* $\{t_{k+1}-t_k, k\in N\}$ *has a positive lower bound.*

Proof. In accordance with (27), for any $t\in[t_k, t_{k+1})$, we have

$$\left|\dot{z}_{p,\delta}(t)\right| \leq \left((2-m/n)k_{1,\delta}\left|e_{p,\delta}(t)\right|^{1-m/n} + (m/n)k_{2,\delta}\left|e_{p,\delta}(t)\right|^{m/n-1} + k_{3,\delta}\right)\left|\dot{e}_{p,\delta}(t)\right| \tag{49}$$

Combined with (25) and (26), we further have

$$\begin{aligned}\left|\dot{z}_{p,\delta}(t)\right| &\leq \left((2-m/n)k_{1,\delta}\left|e_{p,\delta}(t)\right|^{1-m/n} + (m/n)k_{2,\delta}\left|e_{p,\delta}(t)\right|^{m/n-1} + k_{3,\delta}\right)\left|\dot{e}_{p,\delta}(t)\right| \\ &\leq \left((2-m/n)k_{1,\delta}\left|e_{p,\delta}(t)\right|^{1-m/n} + (m/n)k_{2,\delta}\left|e_{p,\delta}(t)\right|^{m/n-1} + k_{3,\delta}\right) \\ &\quad \times\left(k_{1,\delta}\left|e_{p,\delta}(t_k)\right|^{2-m/n} + k_{2,\delta}\left|e_{p,\delta}(t_k)\right|^{m/n} + k_{3,\delta}\left|e_{p,\delta}(t_k)\right| + k_{4,\delta}\right)\end{aligned} \tag{50}$$

As $\left|e_{p,\delta}(t)\right|^{1-m/n}$, $\left|e_{p,\delta}(t)\right|^{m/n-1}$, $\left|e_{p,\delta}(t_k)\right|^{2-m/n}$, $\left|e_{p,\delta}(t_k)\right|^{m/n}$ are all bounded, there must be a positive constant ψ_1 that satisfies

$$(2-m/n)k_{1,\delta}\left|e_{p,\delta}(t)\right|^{1-m/n} + (m/n)k_{2,\delta}\left|e_{p,\delta}(t)\right|^{m/n-1} + k_{3,\delta} \leq \psi_1 \tag{51}$$

and there must be a positive constant ψ_2 that satisfies

$$k_{1,\delta}\left|e_{p,\delta}(t_k)\right|^{2-m/n} + k_{2,\delta}\left|e_{p,\delta}(t_k)\right|^{m/n} + k_{3,\delta}\left|e_{p,\delta}(t_k)\right| + k_{4,\delta} \leq \psi_2 \tag{52}$$

Substituting (51) and (52) into (50), integrating yields

$$\left|z_{p,\delta}(t)\right| \leq \int_{t_k}^{t} \psi_1\psi_2 dT \tag{53}$$

and applying (27)–(29), we have

$$\begin{aligned} z_{p,\delta}(t_{k+1}) &= \rho_{p,\delta}\left(k_{1,\delta}\left|e_{p,\delta}(t)\right|^{2-m/n} + k_{2,\delta}\left|e_{p,\delta}(t)\right|^{m/n} + k_{3,\delta}\left|e_{p,\delta}(t)\right|\right) + k_{4,\delta} \\ &\leq \int_{t_k}^{t_{k+1}} \psi_1\psi_2 dt \\ &= \psi_1\psi_2(t_{k+1} - t_k) \end{aligned} \tag{54}$$

In accordance with (54), we further have

$$\begin{aligned} t_{k+1} - t_k &\geq \frac{\rho_{p,\delta}\left(k_{1,\delta}\left|e_{p,\delta}(t)\right|^{2-m/n} + k_{2,\delta}\left|e_{p,\delta}(t)\right|^{m/n} + k_{3,\delta}\left|e_{p,\delta}(t)\right|\right) + k_{4,\delta}}{\psi_1\psi_2} \\ &\geq \frac{k_{4,\delta}}{\psi_1\psi_2} > 0 \end{aligned} \tag{55}$$

and (55) ensures a positive lower bound for the event-triggered interval to ensure no Zeno behavior. □

4. Simulation Research

In this section, to validate the effectiveness of the proposed control method in this article, simulation experiments will be conducted on a two-joint manipulator with external disturbances and model uncertainties.

The planar model of the manipulator is shown in Figure 2.

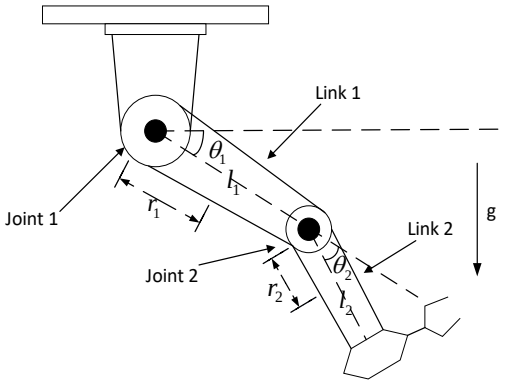


Figure 2. Planar model of the two-link robot, where r_i denotes the distance from the joint $i-1$ to the center of mass of the link i; l_i and m_i respectively denote the length and mass of the link i, where $i = 1, 2$.

Define

$$q = \begin{bmatrix} q_1 \\ q_2 \end{bmatrix} = \begin{bmatrix} \theta_1 \\ \theta_2 \end{bmatrix} \tag{56}$$

By using the Euler–Lagrange equation with the physical parameters of the robot, the correlation matrix of the kinematic equation is described as follows [21]:

$$M(q) = \begin{bmatrix} m_1 r_1^2 + m_2\left(l_1^2 + r_2^2 + 2l_1 r_2 \cos(q_2)\right) + I_1 + I_2 & m_2\left(r_2^2 + l_1 r_2 \cos(q_2)\right) + I_2 \\ m_2\left(r_2^2 + l_1 r_2 \cos(q_2)\right) + I_2 & m_2 r_2^2 + I_2 \end{bmatrix} \tag{57}$$

$$C(q,\dot{q}) = \begin{bmatrix} -m_2 l_1 r_2 \dot{q}_2 \sin(q_2) & -m_2 l_1 r_2 (\dot{q}_1 + \dot{q}_2) \sin(q_2) \\ m_2 l_1 r_2 \dot{q}_1 \sin(q_2) & 0 \end{bmatrix} \tag{58}$$

$$G(q) = \begin{bmatrix} (m_1 r_2 + m_2 l_1) g \cos(q_1) + m_2 r_2 g \cos(q_1 + q_2) \\ m_2 r_2 g \cos(q_1 + q_2) \end{bmatrix} \tag{59}$$

$$J(q) = \begin{bmatrix} -(l_1 \sin(q_1) + l_2 \sin(q_1 + q_2)) & -l_2 \sin(q_1 + q_2) \\ l_1 \cos(q_1) + l_2 \cos(q_1 + q_2) & l_2 \cos(q_1 + q_2) \end{bmatrix} \tag{60}$$

The parameters of the robotic arm are shown in Table 1.

Table 1. The parameters of the manipulator.

Parameter	Description	Value
m_1	Mass of link 1	2.00 kg
m_2	Mass of link 2	0.85 kg
l_1	Length of link 1	0.35 m
l_2	Length of link 2	0.31 m
I_1	Moment of inertia of link 1	0.06125 kgm^2
I_2	Moment of inertia of link 2	0.02042125 kgm^2

To verify the proposed control method, the simulations are achieved with the above manipulator model which compares with the control method proposed in [10]. The initial conditions are set as follows:

$$\begin{cases} q_1(0) = q_2(0) = 0.1 \\ \dot{q}_1(0) = \dot{q}_2(0) = 0 \end{cases} \tag{61}$$

The sampling periods for the two event-trigger conditions proposed in this article are both set to 0.001 s, and the simulation time is set to 40 s. The selection of observer parameters is as follows: $\lambda_1 = 0.01$, $\lambda_2 = 1.2$, $\varepsilon_1 = 1.2$, $\varepsilon_1' = 1$, $\varepsilon_1'' = 1$, $\varepsilon_2 = 1$, $\varepsilon_2' = 1$, $\varepsilon_2'' = 1$, $\gamma = 0.5$. The controller parameter selection is as follows: $k_1 = diag[1,1]$, $k_2 = diag[2.5,2.5]$, $k_3 = diag[0.025,0.025]$, $k_4 = diag[1 \times 10^{-7}, 1 \times 10^{-7}]$, $k_5 = diag[0.0025,0.0025]$, $k_6 = diag[0.025,0.025]$, $k_7 = diag[0.025,0.025]$, $k_8 = diag[1 \times 10^{-9}, 1 \times 10^{-9}]$, $\rho_p = diag[0.1,0.4]$, $\rho_v = diag[0.1,0.4]$, $m = 9$, $n = 13$. The vector of the constrained force $f(t)$ and model uncertainties $\Delta C(x,v)$ and $\Delta G(x)$ is described as follows: $f(t) = \begin{bmatrix} \sin(0.5t)\cos(0.8t) & \cos(0.8t)\cos(0.5t) \end{bmatrix}^T$, $\Delta C(x,v) = 0.2C(x,v)$, $\Delta G(x) = 0.2G(x)$.

The simulation results are shown in Figures 3–12. The trajectory tracking and error of two joints are presented in Figures 3 and 4, which indicates the desired trajectory can be exactly tracked by both controllers within complex disturbance. Although the control method proposed in [10] can converge faster, the controller consumes a significant amount of control effort at the beginning of the response. In Figure 5, the control input is shown. The purple and pink lines denote the proposed inputs, and the blue and red denote the compared control inputs. It can be seen from the figure that the control inputs are within a reasonable and achievable range, proving the feasibility of the controller. Compared with the control methods, the proposed control inputs show more chattering. This phenomenon will be discussed separately later.

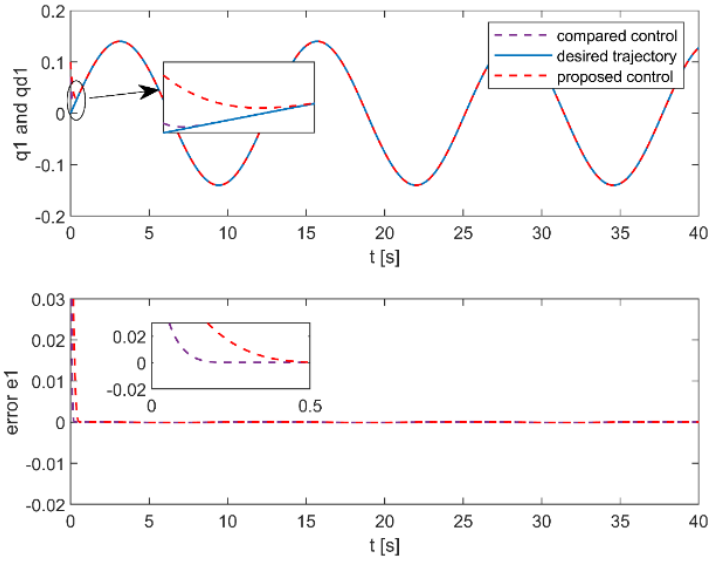


Figure 3. Trajectory tracking and error of joint 1 compared with [10].

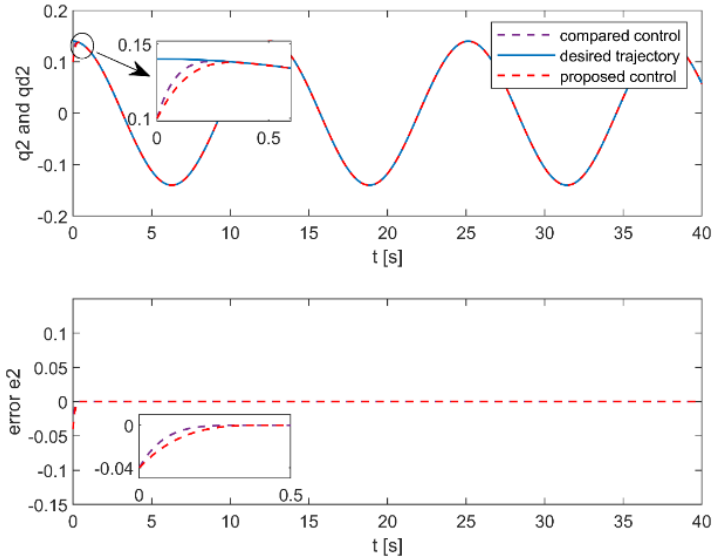


Figure 4. Trajectory tracking and error of joint 2 compared with [10].

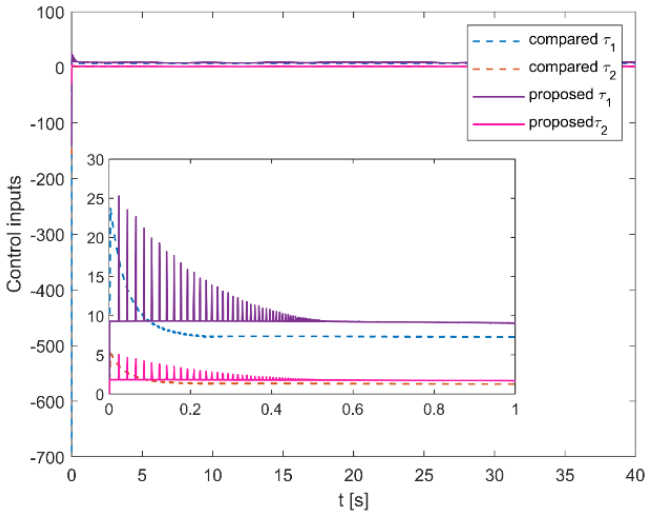


Figure 5. Control input compared with [10].

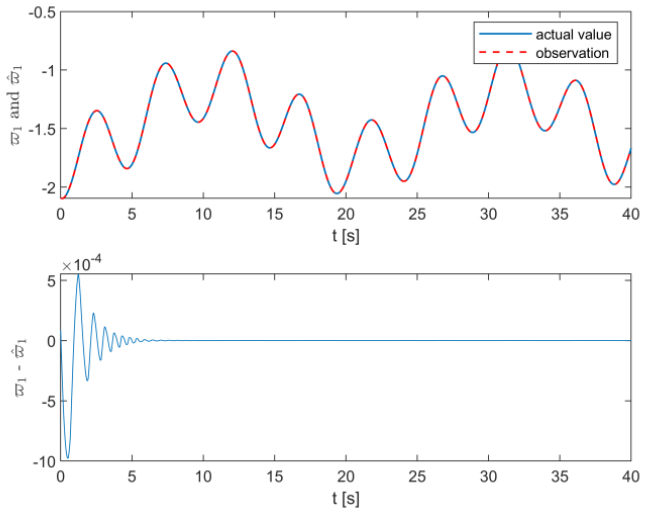


Figure 6. Disturbance and its estimation—joint 1.

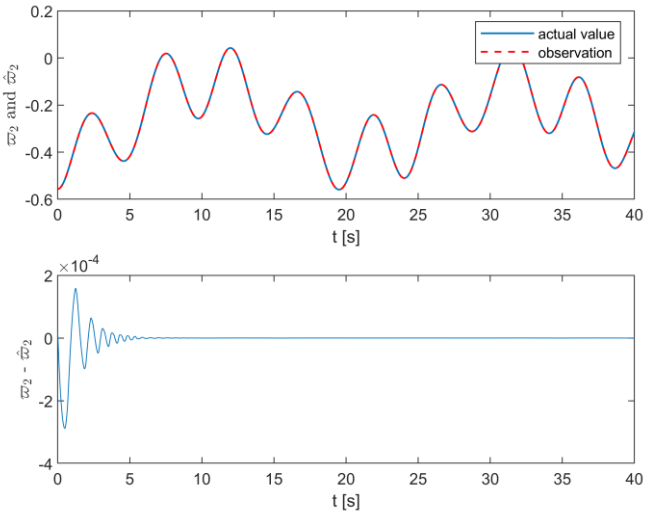


Figure 7. Disturbance and its estimation—joint 2.

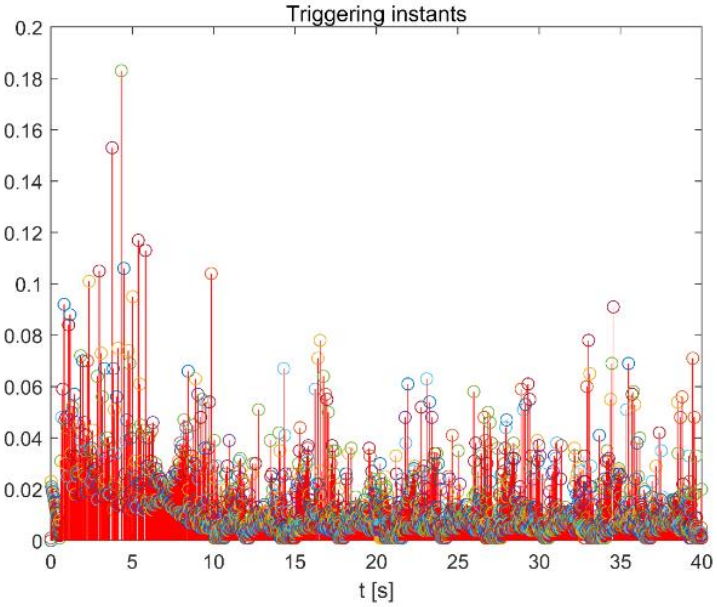


Figure 8. Triggering instants for control input transmission event-time of the manipulator.

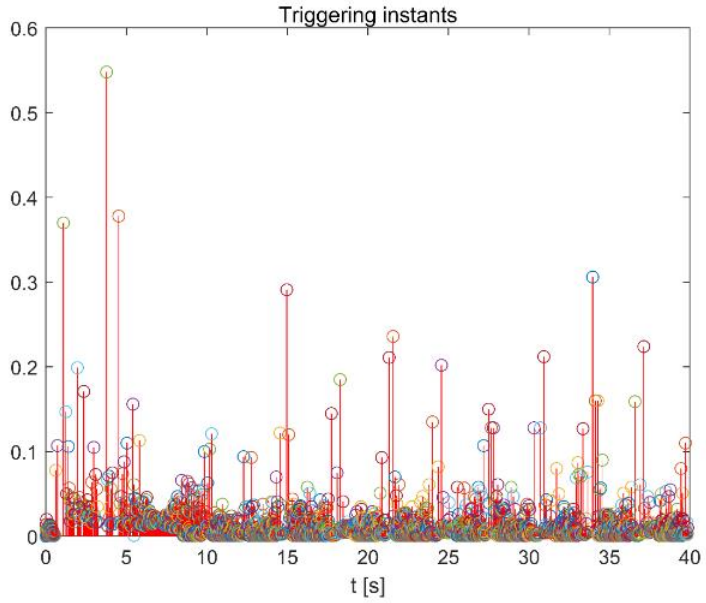


Figure 9. Triggering instants for control output calculation event-time of the manipulator.

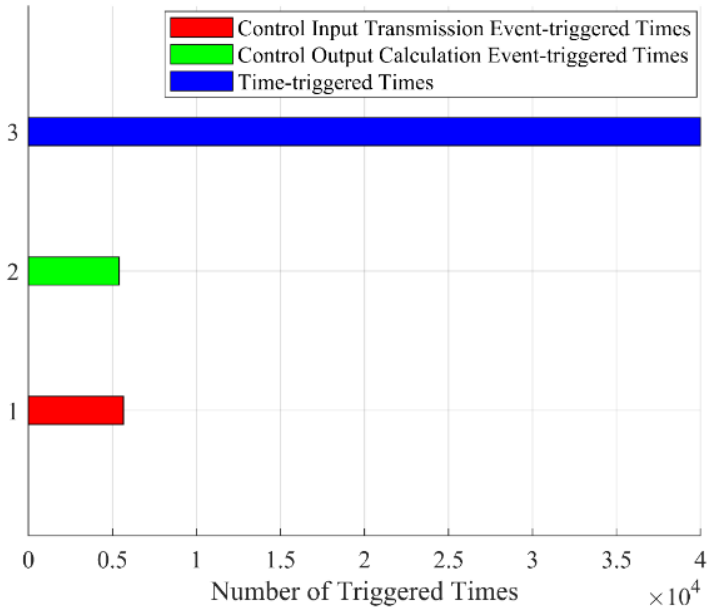


Figure 10. Comparison of the number of triggering times between event-trigger and time-trigger.

The observation effects of the proposed observer are shown in Figures 6 and 7. It is evident from these figures that the observer can accurately reconstruct the lumped disturbances in the system, leading to a precise estimation of these disturbances. Moreover, the observer can stabilize the estimation error within a finite time regardless of the initial state, and the estimation errors are quite small. Specifically, when the system is stable, the estimation error is $|\widetilde{\omega}| \leq 2 \times 10^{-8}$, which also proves that regardless of the initial estimation error, the disturbance observer designed in this article can converge the estimation error to the origin within a fixed time.

Figures 8 and 9 depict the triggering time interval diagrams for the control input transmission and control output calculation of the manipulator, respectively. The horizontal axis denotes the triggered time of the controller, and the vertical axis represents the triggered interval of the controller, which verifies that the event-triggering mechanism proposed in this article effectively reduces the control input transmission time and control output calculation time of the manipulator. To further demonstrate the effectiveness of the designed

event-triggering mechanism in saving resources, we conducted a statistical analysis of the number of event-triggers, as shown in Figure 10. According to the results of Figure 10, the introduction of the event-triggering mechanism can save 85% of control input transmission time and 86% of control output calculation time.

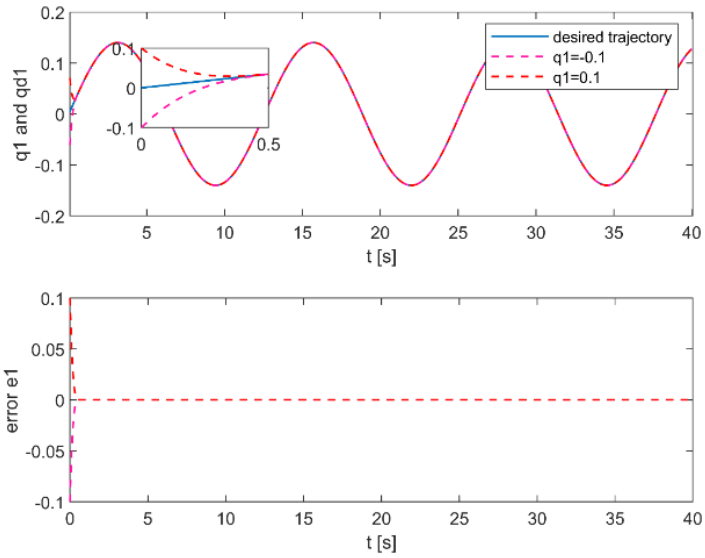


Figure 11. The trajectory tracking of joint 1 and error with different initial states.

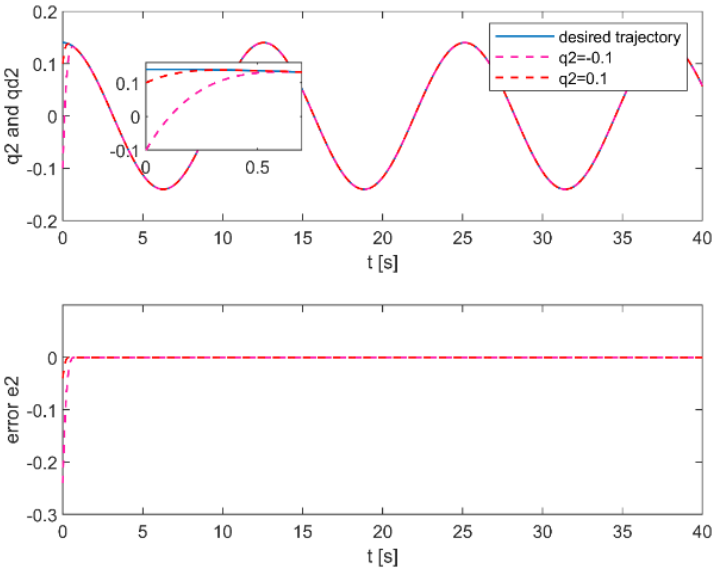


Figure 12. The trajectory tracking of joint 2 and error with different initial states.

In addition, to verify the convergence time of the designed control strategy is independent of the initial state of the system. Depending on the selection of control parameters mentioned above, the upper bound on the convergence time of the manipulator can be calculated as $T_{es} \leq 674$ s. The method proposed in this article will be verified with various initial conditions. We let $q = \begin{bmatrix} 0.1 & 0.1 \end{bmatrix}^T$ and $q = \begin{bmatrix} -0.1 & -0.1 \end{bmatrix}^T$. Figures 11 and 12 validate the effectiveness of the proposed method in this article. With different initial states, the controller can ensure system stability and achieve control objectives within a fixed time.

Based on the above simulation results, the effectiveness of the designed disturbance observer and controller is verified.

5. Discussion

In Figure 5, the proposed control inputs show more chattering than the compared control input; to better analyze the phenomenon, the control input proposed in this article will be compared with the proposed strategy with smaller event-triggering parameters, and the proposed strategy without ETC is shown in Figures 13 and 14. The proposed control strategy with smaller event-triggering parameters is selected as: $\rho_p = diag[0.01, 0.01]$, $\rho_v = diag[0.01, 0.01]$. As shown in Figures 13 and 14, the proposed strategy without ETC shows fewer oscillations compared with the two other control strategies. At the same time, the smaller the event-triggering parameter, the smaller the oscillation range of the control input. Based on the above results, the following conclusions can be drawn:

(1) There is a positive connection between control input oscillation and event-triggering parameters.
(2) The introduction of the ETC mechanism has caused more oscillations, and in practical applications, it is necessary to consider the balance between control input oscillations and reducing data transmission.

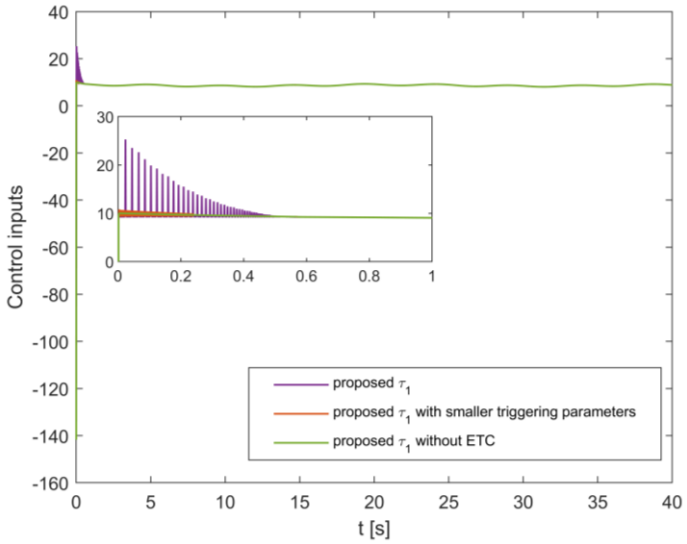


Figure 13. The proposed control input compared with the proposed control strategy with smaller event-triggering parameters and the proposed control strategy without ETC—joint 1.

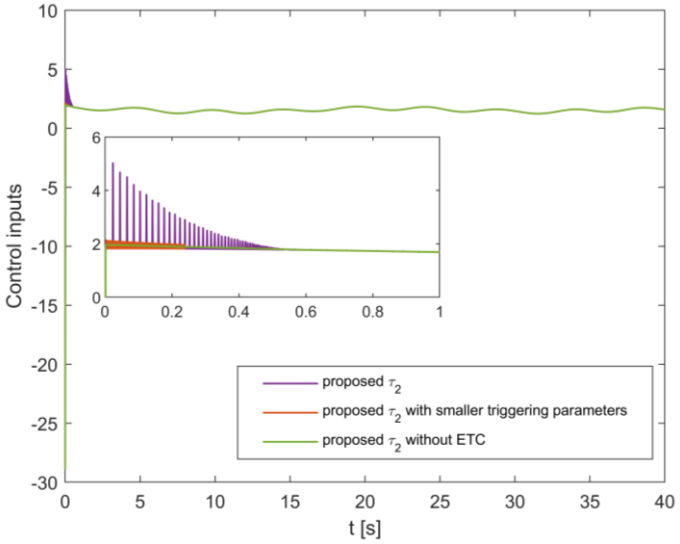


Figure 14. The proposed control input compared with the proposed control strategy with smaller event-triggering parameters and the proposed control strategy without ETC—joint 2.

6. Conclusions

This article studies a fixed-time trajectory tracking control method for an n-joint manipulator based on an event-triggering mechanism. A fixed-time disturbance observer is used to handle system uncertainties, ensuring that the estimation error is stable within a fixed time and independent of the initial estimation error. Based on the framework of backstepping, a fixed-time controller based on an event-triggering mechanism is designed for the manipulator to achieve the control objectives. The controller not only ensures the manipulator tracks the desired trajectory within a fixed time, but also effectively reduces the calculation time of the control output and the transmission time of the control input, and the Zeno behavior is excluded theoretically, simultaneously ensuring the fixed-time stability of the closed-loop system. Furthermore, it is worth noting that the event-triggering mechanism proposed in this article is based on tracking errors rather than control input errors. Compared to event-triggering mechanisms based on control input errors, it has stronger sensitivity. Finally, the effectiveness of the proposed control method is verified through simulation. Given that manipulators typically operate in complex working environments. In future research, we will further study the trajectory-tracking control problem of the manipulator considering actuator saturation.

Author Contributions: Conceptualization, J.P.; data curation, J.P.; formal analysis, G.Z., J.P. and T.L.; funding acquisition, G.Z. and D.W.; investigation, T.L.; methodology, G.Z., J.P. and D.W.; software, J.P. and D.W.; supervision, G.Z.; validation, J.P.; writing—original draft, J.P.; writing—review and editing, G.Z. and D.W. All authors have read and agreed to the published version of the manuscript.

Funding: This research was funded by the Startup Fund for Distinguished Scholars of West Anhui University under Grant No. WGKQ2022050, the Smart Agriculture and Forestry and Smart Equipment Scientific Research and Innovation Team Anhui Undergrowth Crop Intelligent Equipment Engineering Research Center under Grant No. 2022AH010091, and the University Synergy Innovation Program of Anhui Province under Grant No. GXXT-2021-026.

Data Availability Statement: All data used to support the findings of this study are included within the article.

Acknowledgments: The authors would like to thank everyone involved for their contributions to this article. They would also like to thank the editors and anonymous reviewers for their helpful comments and suggestions.

Conflicts of Interest: The authors declare no conflicts of interest.

References

1. Han, L.; Xu, W.; Li, B.; Kang, P. Collision Detection and Coordinated Compliance Control for a Dual-Arm Robot without Force/Torque Sensing Based on Momentum Observer. *IEEE/ASME Trans. Mechatron.* **2019**, *24*, 2261–2272. [CrossRef]
2. Rout, A.; Deepak, B.B.V.L.; Biswal, B.B.; Mahanta, G.B. Weld Seam Detection, Finding, and Setting of Process Parameters for Varying Weld Gap by the Utilization of Laser and Vision Sensor in Robotic Arc Welding. *IEEE Trans. Ind. Electron.* **2022**, *69*, 622–632. [CrossRef]
3. Sun, W.; Wu, Y.; Lv, X. Adaptive Neural Network Control for Full-State Constrained Robotic Manipulator with Actuator Saturation and Time-Varying Delays. *IEEE Trans. Neural Netw. Learn. Syst.* **2022**, *33*, 3331–3342. [CrossRef]
4. Zhu, C.; Yang, C.; Jiang, Y.; Zhang, H. Fixed-Time Fuzzy Control of Uncertain Robots with Guaranteed Transient Performance. *IEEE Trans. Fuzzy Syst.* **2023**, *31*, 1041–1051. [CrossRef]
5. Qiang, J.; Liu, L.; Xu, M.; Fang, Y. Fixed-time backstepping control based on adaptive super-twisting disturbance observers for a class of nonlinear systems. *Int. J. Control* **2021**, *95*, 2294–2306. [CrossRef]
6. Van, M.; Ge, S.S.; Ren, H. Finite Time Fault Tolerant Control for Robot Manipulators Using Time Delay Estimation and Continuous Nonsingular Fast Terminal Sliding Mode Control. *IEEE Trans. Cybern.* **2017**, *47*, 1681–1693. [CrossRef]
7. Xie, Y.; Ma, Q.; Gu, J.; Zhou, G. Event-Triggered Fixed-Time Practical Tracking Control for Flexible-Joint Robot. *IEEE Trans. Fuzzy Syst.* **2023**, *31*, 67–76. [CrossRef]
8. Li, Z.; Su, C.Y.L.; Wang, Z.; Chen, T. Nonlinear Disturbance Observer-Based Control Design for a Robotic Exoskeleton Incorporating Fuzzy Approximation. *IEEE Trans. Ind. Electron.* **2015**, *62*, 5763–5775. [CrossRef]
9. Chen, Z.; Li, Z.; Chen, C.L.P. Disturbance Observer-Based Fuzzy Control of Uncertain MIMO Mechanical Systems with Input Nonlinearities and its Application to Robotic Exoskeleton. *IEEE Trans. Cybern.* **2017**, *47*, 984–994. [CrossRef] [PubMed]

10. Zhang, G.; Pan, J.; Li, T.; Wang, Z.; Wang, D. Fixed-Time Control of a Robotic Arm Based on Disturbance Observer Compensation. *Processes* **2024**, *12*, 93. [CrossRef]
11. Diao, S.Z.; Sun, W.; Su, S.F. Neural-based adaptive event-triggered tracking control for flexible-joint robots with random noises. *Int. J. Robust Nonlinear Control* **2022**, *32*, 2722–2740. [CrossRef]
12. Li, C.; Zhao, L.; Xu, Z. Finite-Time Adaptive Event-Triggered Control for Robot Manipulators with Output Constraints. *IEEE Trans. Circuits Syst. II Express Briefs* **2022**, *69*, 3824–3828. [CrossRef]
13. Ren, H.; Liu, R.; Cheng, Z.; Ma, H.; Li, H. Data-Driven Event-Triggered Control for Nonlinear Multi-Agent Systems with Uniform Quantization. *IEEE Trans. Circuits Syst. II Express Briefs* **2024**, *71*, 712–716. [CrossRef]
14. Priyanka, T.M.C.; Udhayakumar, K.; Mohanrasu, S.S.; Gowrisankar, A.; Rakkiyappan, R. Chaotic synchronization and fractal interpolation-based image encryption: Exploring event-triggered impulsive control in variable-order fractional lur'e systems. *Multimed. Tools Appl.* **2024**, *2024*, 1–40. [CrossRef]
15. Shanmugasundaram, S.; Udhayakumar, K.; Gunasekaran, D.; Rakkiyappan, R. Event-triggered impulsive control design for synchronization of inertial neural networks with time delays. *Neurocomputing*, 2022; 483, 322, 332.
16. Mohanrasu, S.S.; Udhayakumar, K.; Priyanka, T.M.C.; Gowrisankar, A.; Banerjee, S.; Rakkiyappan, R. Event-Triggered Impulsive Controller Design for Synchronization of Delayed Chaotic Neural Networks and Its Fractal Reconstruction: An Application to Image Encryption. *Appl. Math. Model.* **2023**, *115*, 490–512. [CrossRef]
17. Cui, G.; Yang, W.; Yu, J.; Li, Z.; Tao, C. Fixed-Time Prescribed Performance Adaptive Trajectory Tracking Control for a QUAV. *IEEE Trans. Circuits Syst. II Express Briefs* **2022**, *69*, 494–498. [CrossRef]
18. Pan, Y.; Du, P.; Xue, H.; Lam, H.K. Singularity-Free Fixed-Time Fuzzy Control for Robotic Systems with User-Defined Performance. *IEEE Trans. Fuzzy Syst.* **2021**, *29*, 2388–2398. [CrossRef]
19. Van, M.; Sun, Y.; Mcllvanna, S.; Nguyen, M.N.; Khyam, M.O.; Ceglarek, D. Adaptive Fuzzy Fault Tolerant Control for Robot Manipulators with Fixed-Time Convergence. *IEEE Trans. Fuzzy Syst.* **2023**, *31*, 3210–3219. [CrossRef]
20. Liang, X.L.; Wang, H.B.; Zhang, Y.X. Adaptive nonsingular terminal sliding mode control for rehabilitation robots. *Comput. Electr. Eng.* **2022**, *99*, 107718. [CrossRef]
21. He, W.; Ge, S.S.; Li, Y. Neural Network Control of a Rehabilitation Robot by State and Output Feedback. *J. Intell. Robot. Syst.* **2015**, *80*, 15–31. [CrossRef]
22. Sui, W.; Duan, G.; Hou, M.; Zhang, M. Distributed fixed-time attitude coordinated tracking for multiple rigid spacecraft via a novel integral sliding mode approach. *J. Frankl. Inst.* **2020**, *357*, 9399–9422. [CrossRef]
23. Tian, B.; Zuo, Z.; Yan, X.; Wang, H. A fixed-time output feedback control scheme for double integrator systems. *Automatica* **2017**, *80*, 17–24. [CrossRef]
24. Polyakov, A. Nonlinear Feedback Design for Fixed-Time Stabilization of Linear Control Systems. *IEEE Trans. Autom. Control* **2012**, *57*, 2106–2110. [CrossRef]
25. Zou, A.; Ruiter, A.; Kumar, K. Distributed finite-time velocity-free attitude coordination control for spacecraft formations. *Automatica* **2016**, *67*, 46–53. [CrossRef]
26. Xuan-Mung, N.; Golestani, M. Energy-Efficient Disturbance Observer-Based Attitude Tracking Control with Fixed-Time Convergence for Spacecraft. *IEEE Trans. Aerosp. Electron. Syst.* **2023**, *59*, 3659–3668. [CrossRef]

Disclaimer/Publisher's Note: The statements, opinions and data contained in all publications are solely those of the individual author(s) and contributor(s) and not of MDPI and/or the editor(s). MDPI and/or the editor(s) disclaim responsibility for any injury to people or property resulting from any ideas, methods, instructions or products referred to in the content.